processes

MDPI

Article

Revealing of Supercritical Water Gasification Process of Lignin by Reactive Force Field Molecular Dynamics Simulations

Veerapandian Ponnuchamy [1,2,*], Jakub Sandak [1,2] and Anna Sandak [1,3]

[1] InnoRenew CoE, Livade 6, 6310 Izola, Slovenia; jakub.sandak@innorenew.eu (J.S.); anna.sandak@innorenew.eu (A.S.)
[2] Andrej Marušič Institute, University of Primorska, Titrov trg 4, 6000 Koper, Slovenia
[3] Faculty of Mathematics, Natural Sciences and Information Technologies, University of Primorska, Glagoljaška 8, 6000 Koper, Slovenia
* Correspondence: veerapandian.ponnuchamy@innorenew.eu; Tel.: +386-(0)40-282-944

Abstract: Gasification with supercritical water is an efficient process that can be used for the valorization of biomass. Lignin is the second most abundant biopolymer in biomass and its conversion is fundamental for future energy and value-added chemicals. In this paper, the supercritical water gasification process of lignin by employing reactive force field molecular dynamics simulations (ReaxFF MD) was investigated. Guaiacyl glycerol-β-guaiacyl ether (GGE) was considered as a lignin model to evaluate the reaction mechanism and identify the components at different temperatures from 1000 K to 5000 K. The obtained results revealed that the reactions and breaking of the lignin model started at 2000 K. At the primary stage of the reaction at 2000 K the β-O-4 bond tends to break into several compounds, forming mainly guaiacol and 1,3-benzodioxole. In particular, 1,3-benzodioxole undergoes dissociation and forms cyclopentene-based ketones. Afterward, dealkylation reaction occurred through hydroxyl radicals of water to form methanol, formaldehyde and methane. Above 2500 K, H_2, CO and CO_2 are predominantly formed in which water molecules contributed hydrogen and oxygen for their formation. Understanding the detailed reactive mechanism of lignin's gasification is important for efficient energy conversion of biomass.

Keywords: gasification; super-critical water; lignin; reactive force field molecular dynamics simulations

check for updates

Citation: Ponnuchamy, V.; Sandak, J.; Sandak, A. Revealing of Supercritical Water Gasification Process of Lignin by Reactive Force Field Molecular Dynamics Simulations. *Processes* **2021**, *9*, 714. https://doi.org/10.3390/pr9040714

Academic Editor: Andrea Pizzi

Received: 31 March 2021
Accepted: 16 April 2021
Published: 18 April 2021

Publisher's Note: MDPI stays neutral with regard to jurisdictional claims in published maps and institutional affiliations.

Copyright: © 2021 by the authors. Licensee MDPI, Basel, Switzerland. This article is an open access article distributed under the terms and conditions of the Creative Commons Attribution (CC BY) license (https://creativecommons.org/licenses/by/4.0/).

1. Introduction

Biomass is a complex mixture of carbon-based organic molecules containing hydrogen, oxygen, often nitrogen and also small quantities of other atoms. Lignocellulosic biomass as a fuel is age-old and most widely used, cheap, abundantly available, clean (biomass has no sulfur content and has a short CO_2 fixation cycle), moreover, is renewable and sustainable [1]. On the other hand, biomass has high water and ash content, low heating value, is heterogeneous and difficult to transport. Extensive interest in the utilization of bio-resources for bioenergy, biopolymers, bio-fuels and other bio-materials production is observed all over the world [2]. If properly managed, the renewable feedstock can replace a significant amount of current petroleum consumption. The EU target for renewable energy consumption is raised to 32% by 2030, from 20% in 2020 [3]. This number can be extended even more if additional natural resources and agricultural/forest areas will be cultivated with suitable plants. The utilization of biomass has become a very important issue due to the uncertain supply of non-renewable resources (such as oil/coal) and increased recognition of the environmental problems related to global warming and pollutions [4].

The uses of biomasses are dependent, however, on these specific characteristics. Many physico-chemical, structural and compositional factors complicate the biomass conversion processes. Heterogeneity is a natural property of biomass, which is difficult to control but possible to monitor [5]. Therefore, to properly convert biomass, it is extremely important to know at the early stage the full characteristics including chemical, physical, or energetic

properties. The chemical composition of biomass includes carbohydrates (cellulose, hemicellulose, simple sugars), lignin, extractives, water and ash forming constituents. All of them influence the properties of biomass and their conversion. Cellulose is the structural component of a green plant's cell walls. It is comprised of carbon, hydrogen and oxygen and is the most abundant organic material on earth. Hemicellulose has a share of 20% to 40%, occurs in association with cellulose and is chemically bonded to lignin. Hemicellulose consists of short, highly branched, chains of sugars. It contains five-carbon sugars (usually D-xylose and L-arabinose), six-carbon sugars (D-galactose, D-glucose and D-mannose) and uronic acid [6]. Lignin is a complex structure of phenyl propane units linked primarily by ether bonds. This polymer gives plants their structural integrity and is not easily degraded. The composition and amount of lignin vary from species to species, tree to tree and even in woods from different parts of the same tree [7]. Softwoods are known to contain higher contents of lignin, followed by hardwoods and grasses. Moreover, lignin from hardwood contains higher methoxyl content due to the presence of an approximately equal number of guaiacyl and syringyl units. On the other hand, around 90% of the total units of lignin derivate from softwood is guaiacyl [8]. Lignin offers a significant opportunity for enhancing the operation of a lignocellulosic biorefinery since it is an extremely abundant raw material contributing as much as 30% of the weight and 40% of the energy content of lignocellulosic biomass. Lignin's native structure suggests that it could play a central role as a new chemical feedstock, particularly in the formation of supramolecular materials and aromatic chemicals [9]. Lignin decomposes between 280 °C and 500 °C. Char is the more abundant constituent in the products of lignin pyrolysis with a yield of 55%. A liquid product known as pyroligneous acid consists of 20% aqueous components and 15% tar residue on dry lignin basis. The gaseous products represent 10% of the lignin decomposition products and are composed of methane, ethane and carbon monoxide [10].

Lignin is an aromatic polymer, containing many cross-linked macromolecules (molecular masses above 10,000 au) which are difficult to gasify [11]. Gasification is a high-temperature thermochemical conversion process focused on the production of combustible gas, instead of heat. This is achieved through the partial combustion of the biomass material in a restricted supply of air or oxygen, usually in a high-temperature environment. Gasification takes place in two main stages. First, the biomass is partially burned to form producer gas and charcoal. In the second stage, the carbon dioxide and water produced in the first stage are chemically reduced by charcoal, forming carbon monoxide and hydrogen.

One of the most promising methods for thermochemical conversion of biomass into hydrogen-rich gas is the gasification of lignin in supercritical water [12–14]. In this method, wet biomass can be converted into hydrogen-rich syngas at lower and higher temperatures with different catalysts. The higher efficiency of the process is due to the high dispersion and effective heat transfer of water in its supercritical condition (374 °C, 22.1 MPa) [15,16]. Water in Supercritical Water Gasification acts as a reaction medium and reactant. A major part of biomass is solved and reformed through a homogeneous mixture. According to Calzavara et al., 2005 water–gas shift (producing H_2 and CO_2 from CO and H_2O) and methanation (producing CH_4 and H_2O from CO and H_2) reactions occur with biomass reforming in supercritical water simultaneously [17]. As a result, the number of by-products (such as char and tar) is minimized, leading to higher gas yields [18]. The main challenge for Supercritical Water Gasification (SCWG) of lignin is process efficiency; therefore, the use of catalysts is often suggested [18]. The yield of product gases (H_2, CH_4, CO and CO_2) is closely linked to reaction rates along competing pathways. The common goal for biomass gasification is maximizing H_2 production by the optimization of reaction temperatures, residence times and selected catalysts [19]. Yoshida et al., 2001, 2003 showed that the hydrogen yield by SCWG of the cellulose and hemicellulose are higher than that of lignin. The hydrogen yield of lignin depends on the species and the interaction between each biomass component [20,21].

Reactive force field (ReaxFF) is a bond order-based force field developed for molecular dynamics simulations to deal with a few hundred atoms and provide a clear insight

about bond breaking and bond-forming during the simulations. This force field was originally developed by van Duin and Gooddard et al. [22]. ReaxFF methods have been successfully employed to study the gasification of organic molecules under a supercritical water environment [23–25]. Similarly, the pyrolysis of biomass and lignin and gasification of lignin with supercritical water were investigated [26–29]. Li et al. comprehensively illustrated the lignin gasification in supercritical water and reported the pathway to produce three main products such as H_2, CO_2 and CH_4. During the gasification process, the typical bond, C-O-C is broken first and followed by C-C bonds in aromatic ring structures [30]. On the other hand, Han et al. investigated the effect of Ni nanoparticles as a catalyst to evaluate the bond breaking in the β-O-4 lignin model and stated that Ni catalyst could potentially break the C-O bond and dissociate the conjugated π bond in the aromatic ring. The 2.0 nm size of Ni catalyst showed a greater performance than 3.0 nm and 4.0 nm due to larger surface area and lower surface oxidation degree [31]. Recently, the lignin γ-O-4 model was studied in supercritical water between 2000 K to 6000 K temperatures and reported the H_2 and CO gases are predominantly generated and H_2O molecules contribute H and O abundantly for those gases [32]. The present research focuses mainly on the most dominant β−O−4 linkage without the presence of any catalyst. Although the aforementioned studies with the β−O−4 model have extensively investigated the production of syngas molecules, the intermediate value-added chemicals from lignin are still remaining unclear. Therefore, this study investigates the lignin model from temperature 1000 K to 5000 K to elaborate step-by-step evolution of products in supercritical water.

2. Computational Details

The present work focusses on the investigation of the β-O-4 lignin model as this particular linkage presents over half of the other linkages (α-O-4, β-β, β-1 and 5-5′) in the lignin macromolecule [33]. Guaiacyl glycerol-β-guaiacyl ether (GGE - $C_{17}H_{20}O_6$) is the typical lignin model compound representing β-O-4 linkages and contains guaiacyl units and hydroxyl groups located at α- and γ- position (Figure 1a). Before performing ReaxFF simulations, the isolated geometry was optimized using wB97X-D/6-311g(d,p) level of theory as described in the reference [34] using GAMESS code [35]. The GGE model has been used successfully for various studies, including dissolution of lignin, using different solvents [36,37], catalytic cleavage reactions [38–41] and pyrolysis [42–44].

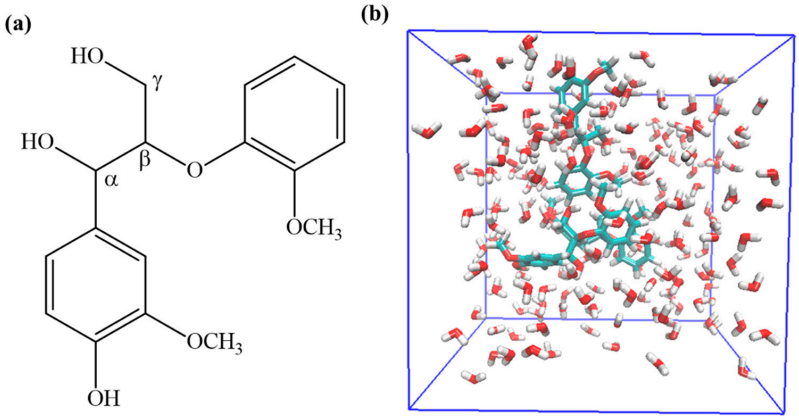

Figure 1. (**a**) Lignin model—Guaiacyl glycerol-β-guaiacyl ether (GGE) (**b**) The simulation box contains three GGE and 200 water molecules.

The simulation box was constructed with three GGE models with 200 water molecules using Packmol (18.169, University of São Paulo, Brazil, 2009) [45] and the setup is shown in Figure 1b. The present study used the force field parameters as reported in the literature [46]. The ReaxFF simulations were performed using the LAMMPS (12Dec18, Sandia National Labs- Albuquerque, New Mexico, USA and Temple University-Philadelphia, Pennsylvania, USA, 1995) package by incorporating reax/c pair_style. First, the simulation box was

minimized and followed by isothermal-isobaric (NPT) ensemble simulation for 1 ps with a temperature of 200 K. The initial density of the system is around 0.4219 g cm^{-3} with a box size of 26.08 Å × 26.08 Å × 26.08 Å and periodic boundary condition was adopted. Before studying the system at the higher temperature, the system was again equilibrated for 2.5 ps at 300 K using Berendsen thermostat. Afterward, the temperature of the system was heated to 1000 K, 1500 K, 2000 K, 2500 K, 3500 K, 4000 K, 4500 K and 5000 K to study and evaluate the chemical components. 0.1 fs timestep was employed for all simulations up to 1 ns and trajectory was written every 10 fs for post-analysis. The evolution of radicals and reaction networks was analyzed with the efficient tool, called ReacNetGenerator [47].

3. Results and Discussion

3.1. The Impact of Low Temperatures: 1000 K and 1500 K

Before applying a higher temperature for lignin gasification, two simulations were investigated with the temperature of 1000 K and 1500 K to study initial reactions potentially occurring at low temperature. The number of molecules such as water and lignin model were analyzed and it was predicted that water molecules and lignin models remain almost the same for about 1 ns. This particular observation clearly indicates that no reactions can be initiated at the 1000 K and 1500 K temperature.

3.2. At Temperature 2000 K

There are three possible reactions that can occur with increasing temperatures such as water molecules degradation alone, the reaction between water-lignin molecules and lignin degradation alone. These possible reactions were analyzed and the number of water molecules at 2000 K along with hydroxyl radicals is illustrated in Figure 2. The plausible reaction scheme of lignin degradation is demonstrated in Figure 3. Around 0.1 ns, the dissociation of the lignin model compound has occurred between the most fragile β-O-4 linkage and form compound 1 and compound 10. These corresponding radicals react with water and result in compound 2 and compound 11. The fragment analysis showed that there are some intermediates formed such as H_4O_2 (water dimer), H_3O_2 (H-O-H- - - O-H) along with OH radicals. However, we obtained higher water molecules (201 in total) in the range between 0.8 and 0.9 ns which is due to the fact of dissociation of methoxy and alkyl side chains in the lignin model into main products like, CH_3OH and HCHO and formed OH radicals absorb protons from lignin model into H_2O molecules. Furthermore, there are two possible reactions that occurred in lignin model (i) reaction between α-OH and β-H (ii) γ-OH and β-H to form compound 11 (Figure 3) by elimination of OH radicals which eventually form H_2O in the following step. Compound 11 is one of the building blocks of lignin monomer, coniferyl alcohol. The methoxy groups present in the aromatic rings are relatively stable during the first pyrolysis reaction, however, they undergo breaking into isolated menthol molecules [48] in the successive pyrolysis reaction.

It is very interesting to see that the typical lignin model is predominantly formed of 4-methoxy substituted phenols (compound **2**) or guaiacol at the primary stage of the gasification of lignin (Figure 4a). This result is in good agreement with the work described by Kawamoto [48]. In addition, the compound 1 radical can form a compound 3 which is known as 1,3-benzodioxole and is one of the products evolved at 2000 K. The 1,3-benzodioxole can be used as ingredients for fragrance industries and as a protective group in synthetic organic chemistry [49,50]. However, it can be seen in Figure 3 that it undergoes bond breaking and rearrangements and forming of compounds **5** and **6** which could lead to the formation of cyclopentenone (compound **8**) and methyl-cyclopentanone (compound **9**). In the case of compound 2, a dealkylation reaction was occurred to form compound **4**, which is known as catechol and it further degrades to phenol. During the simulation, the evolution profile of compounds such as 2, 3, 5 and 12 have been extracted and shown in Figure 4. As can be seen from Figure 4b,c, 1,3-benzodioxole was formed at below 0.6 ns and afterwards. This compound 3 can be dissociated into compound 5 in which the amount of

compound **5** was increasing from about 0.6 ns and stays until 1 ns. This is also confirmed that the cyclopentene-based compounds can be obtained from 1,3-benzodioxole.

It is stressed that the recent study unraveled several identified relative components of the guaiacol in supercritical water at different reaction times and found a 1,3-benzodioxole (compound **3**) below the 60s during gasification using gas chromatography/mass spectrometry (GC/MS) [51]. On the other hand, the same authors, Cao et al. and Miliotti et al. have predicted the formation of cyclopentanone (compound **8**) and 2-cyclopentanone (compound **9**) when treating lignin with supercritical water [51–53]. Even if, any of these compounds **8** and **9** can be formed during the present simulations, we believe that these compounds can be extracted through controlled experimental gasification of lignin with supercritical water.

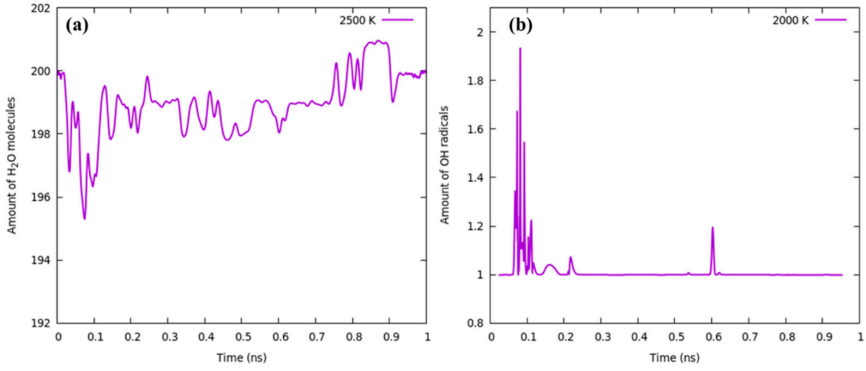

Figure 2. (**a**) Total number of water molecules (**b**) Amount of OH (hydroxy) radicals at 2000 K.

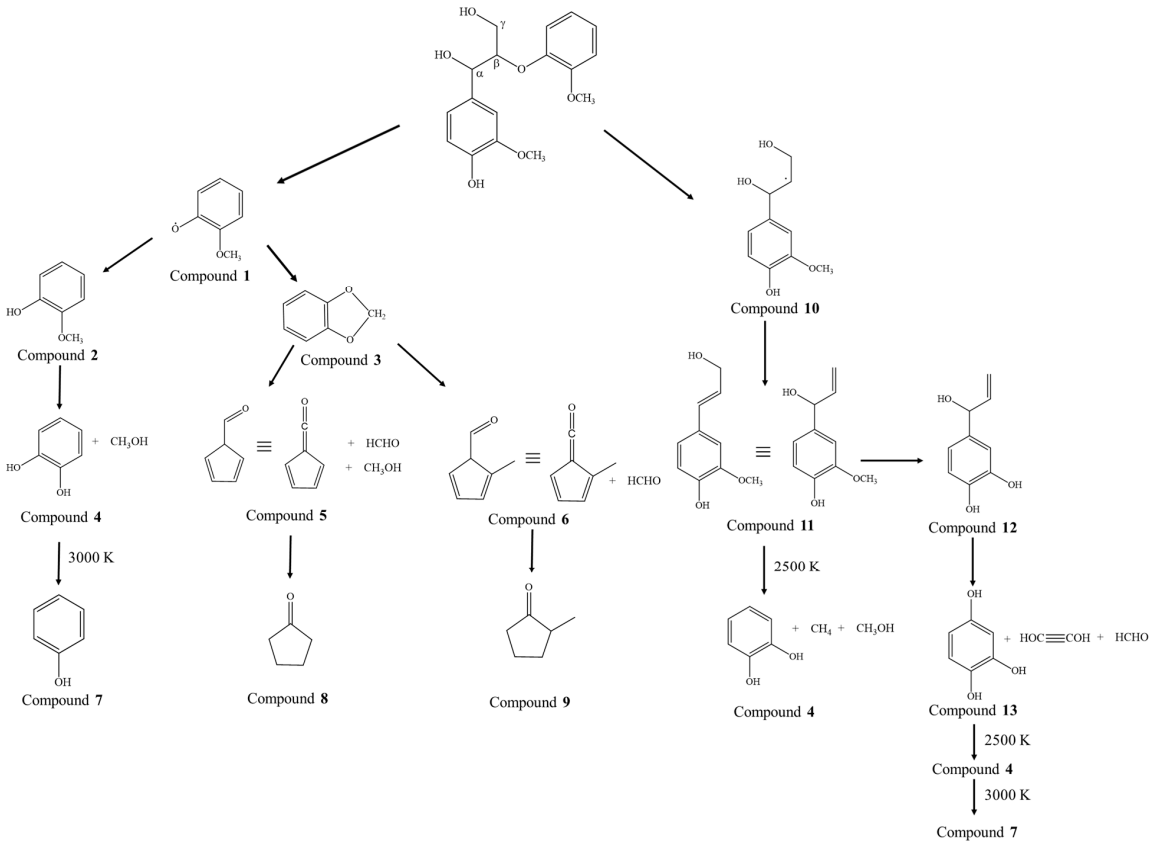

Figure 3. The schematic representation of major reaction components at 2000 K.

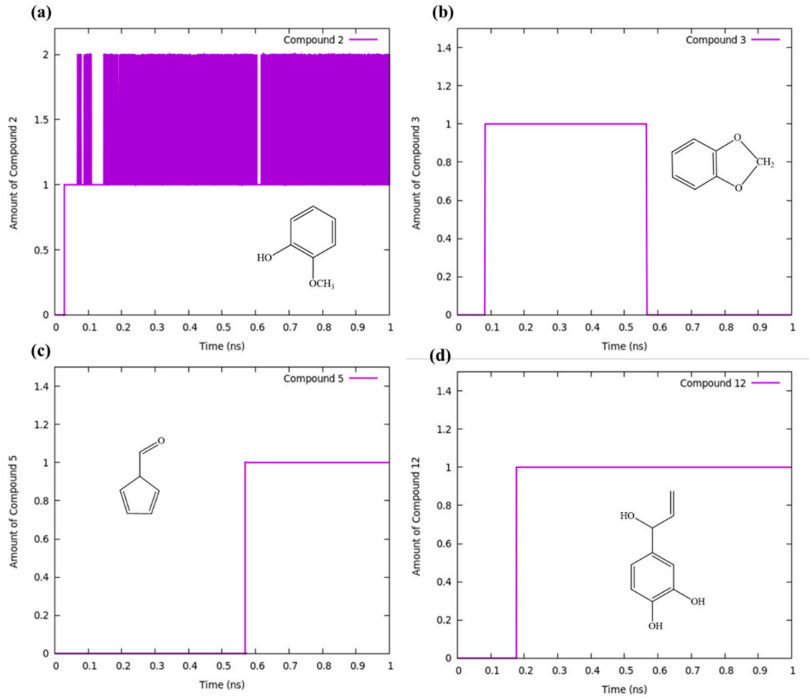

Figure 4. The number of compounds (**a**) compound **2**, (**b**) compound **3**, (**c**) compound **5** and (**d**) compound **12** evolved at a temperature of 2000 K.

3.3. 2500 K and Higher Temperature

During the gasification of lignin, several compounds have been identified concerning different temperatures employed. The most dominant molecules with several concentrations are shown in Figure 5. With an increase of temperature, the number of water molecules decreased due to the formation of H and OH reactive radicals. At 5000 K, the number of total H_2O molecules is about 150. The active OH radicals dealkylate lignin molecules and form formaldehyde compound (Figure 5b). Several authors have reported the formation of formaldehyde molecules by treating lignin with base and acid-based reagents [54–56]. Moreover, Toledano et al., have attempted to entrap the active formaldehyde molecules to avoid lignin repolymerization [55]. Although formaldehyde molecules are reactive, they dissociate at increasing temperatures into CO and H_2. Methoxy groups in the aromatic ring are hydrolyzed with water into methanol and a higher concentration of these molecules is obtained at 2500 K (Figure 5c). However, over 2500 K, the concentration decreases due to degradation to methyl and ethylene radicals. The formed methyl radicals absorb H radicals from water at higher than 2000 K to form methane molecules. This process was not observed at a lower temperature than 2000 K. Afterwards, the number of methane molecules increased until 3500 K and dropped at higher temperature due to the dissociation of methane to H_2 and CO. Similar trend was also observed for ethylene molecules (Figure 5e). Comparing the gases such as CO_2, H_2 and CO in Figure 5f–h, the higher the number of syngas (H_2 and CO) was formed at the higher temperature. It is interesting to observe that no syngas was noticed at the temperature of 2000 K and a low amount of those molecules are predominant at 2500 K due to low dissociation. The observed number of CO and H_2 molecules are consistent with the recent gasification study of γ-O-4 using ReaxFF [32]. In particular, the H_2 molecules were generated from the water molecules present in the system through intermediate H radicals that evolved from water. The trend evidencing the amount of water and H_2 is presented in Figure 5a,g, where water molecules decrease at the higher temperature. Simultaneously the generation of amount H_2 molecules increases. The evolution of CO_2 molecules can be seen from 3000 K because it is mainly generated from aromatic rings which required higher temperature for dissociation. Figure 6 demonstrates the number of hydroxyl, methyl and formaldehyde radicals formed

at different temperatures employed in the simulation. The increasing temperature breaks water molecules more into radicals such as H and OH which greatly participate in the breaking of methoxy groups and hydroxyl groups present in the lignin. The more reactive methyl and formaldehyde radicals are formed at increasing temperature up to 3500 K. The methyl radicals belong to the aromatic methoxy group which undergoes cleavage at the second stage of the pyrolysis (after β-O-4 bond-breaking process) which then absorbs H or HO radicals from water to form methane or methanol respectively. At higher temperatures, it eventually produced H_2 and CO gases. Similarly, formaldehyde radicals' formation may originate from the hydroxyl alkyl chain of the lignin model (α-C or γ-C atoms) which lead to the formation of formaldehyde molecules before subjected to form syngas molecules at a higher temperature.

The main reaction pathways with radicals' formation and reaction with other molecules are illustrated in Table 1. The presented reaction scheme is different from what the other authors have proposed in their works [30–32]. They elaborated the most possible generation of CO and H_2 molecules which are not taken into account in Table 1. The present work considers the formed compounds and intermediates to generate CO and H_2. During the simulations, several other compounds have been identified such as HCOOH, H_2O_2, CH_4, CH_3OH, C_2H_4 and $C_2H_4O_2$. These compounds have exhibited series of reactions with radicals like H and HO to form final syngas molecules (H_2 and CO) as well as CO_2. Comparing the Figures 5 and 6 with Table 1, it can be seen that most of the syngas molecules formed from H and O excelled from water molecules. On the other hand, few numbers of short alkanes like methane and CO_2 are generated from the lignin model. These identified components are consistent with the results obtained in different simulations with lignin [30–32].

Table 1. The main pathways of generation of different radicals and gases.

H_2O			→	H·	+	HO·
2 H·			→	H_2		
HCOOH			→	HCOO·	+	H·
HCOO·			→	CO_2	+	H·
HCOO·			→	CO	+	HO·
HCOO·	+	H·	→	CO_2	+	H_2
HCOO·	+	OH·	→	CO_2	+	H_2O
H_2O_2			→	HOO·	+	H·
H_2O_2			→	O_2	+	H_2
H_2O_2			→	2 HO·		
CH_4	+	OH·	→	CH_3·	+	H_2O
CH_3·	+	H·	→	CH_2··	+	H_2
CH_2··			→	C_2H_4		
CH_3·	+	H_2	→	CH_4	+	H·
CH_3·	+	H_2O	→	CH_3OH	+	H·
CH_3OH	+	HO·	→	$[CH_2OH]$ ·	+	H2O
CH_3OH	+	H·	→	$[CH_2OH]$ ·	+	H_2
$[CH_2OH]$ ·	+	H_2	→	CH_4	+	HO·
$[CH_2OH]$ ·	+	H_2O	→	CH_3O·	+	HO·
CH_3O·	+	H·	→	CO	+	$2H_2$
HO-C≡C-OH	+	4 H·	→	·C≡C·	+	2 H_2O
·C≡C·	+	2 H·	→	HC≡CH		
HC≡CH	+	2 H·	→	$H_2C=CH_2$		
H2C=CH2	+	4 H·	→	2 CH_4		
CH_4	+	H_2O	→	CO	+	6 H_2

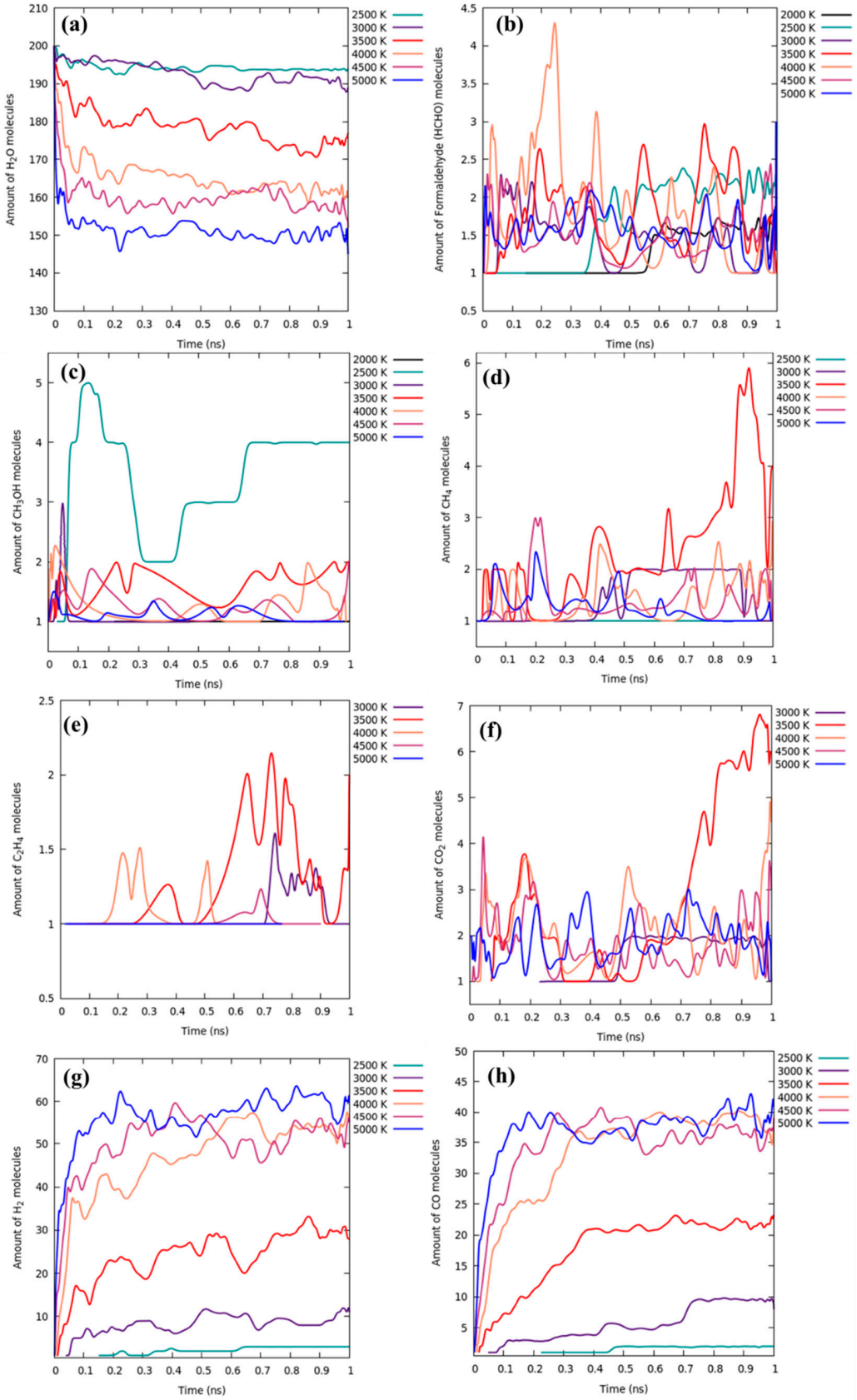

Figure 5. The number of the most dominant molecules: (**a**) Water, (**b**) Formaldehyde, (**c**) Methanol, (**d**) Methane, (**e**) Ethylene, (**f**) CO_2, (**g**) H_2 and (**h**) CO at different temperatures.

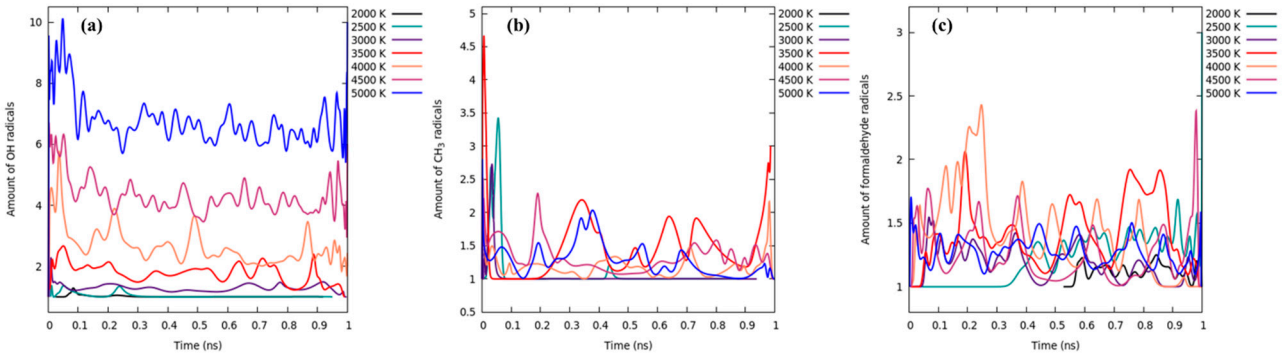

Figure 6. Total number of, (**a**) hydroxyl radicals (**b**) methyl radicals and (**c**) formaldehyde radicals at different temperatures.

4. Conclusions

The reactive force field molecular dynamics simulations (ReaxFF) method was employed to evaluate the gasification process of the lignin model in supercritical water. The guaiacyl glycerol-β-guaiacyl ether model is considered for the lignin model and 9 different temperatures were studied between 1000 K to 5000 K. It was observed that no change was noticed in the amount of water and lignin molecules at 1000 K and 1500 K, which proofs that no reactions were initiated. At 2000 K, the primary stage reaction has occurred and cleavage of β-O-4 bond into the formation of guaiacol, 1,3-benzodioxole and coniferyl alcohol. The component analysis results showed that 1,3-benzodioxole further leads to cyclopentene-based ketone. Afterward, dealkylation reactions at the benzyl methoxy group occurred. The increasing temperature results in more dissociation of water to hydrogen and hydroxyl radicals which significantly influence syngas production. It is estimated that mostly water contributed to the formation of HO, CO and CH_4 gases. The presented results provide a detailed analysis that can assist to extract the value-added chemicals and syngas by employing different temperatures.

Author Contributions: Conceptualization, V.P., J.S. and A.S.; methodology, V.P.; software, V.P.; validation, V.P.; formal analysis, V.P.; investigation, V.P.; resources, V.P.; data curation, V.P.; writing—original draft preparation, V.P., J.S. and A.S.; writing—review and editing, V.P., J.S. and A.S.; visualization, V.P.; supervision, V.P. All authors have read and agreed to the published version of the manuscript.

Funding: The authors gratefully acknowledge the European Commission for funding the InnoRenew project (Grant Agreement #739574) under the Horizon2020 Widespread-Teaming program, the Republic of Slovenia (investment funding from the Republic of Slovenia and the European Union's European Regional Development Fund) and infrastructural ARRS program IO-0035.

Institutional Review Board Statement: Not applicable.

Informed Consent Statement: Not applicable.

Data Availability Statement: Not applicable.

Acknowledgments: Part of this work was conducted during project HYGRO-WOOD (BI-LT/20-22-002) funded by ARRS.

Conflicts of Interest: The authors declare no conflict of interest.

References

1. Ahorsu, R.; Medina, F.; Constantí, M. Significance and Challenges of Biomass as a Suitable Feedstock for Bioenergy and Biochemical Production: A Review. *Energies* **2018**, *11*, 3366. [CrossRef]
2. Lebaka, V.R. Potential Bioresources as Future Sources of Biofuels Production: An Overview. *Biofuel Technol.* **2013**, 223–258. [CrossRef]
3. Commodities 2021: Climate Change Policy Targets to Stimulate EU Biodiesel Consumption | S&P Global Platts. Available online: https://www.spglobal.com/platts/en/market-insights/latest-news/agriculture/122320-commodities-2021-climate-change-policy-targets-to-stimulate-eu-biodiesel-consumption (accessed on 24 March 2021).

4. Sandak, A.; Sandak, J. Utilization of FT-NIR for Proper Biomass Conversion. In Proceedings of the NIR2013-A1—Agriculture, Environment, La Grande-Motte, France, 2 June 2013.
5. Anukam, A.; Berghel, J. Biomass Pretreatment and Characterization: A Review. *Biomass* **2020**. [CrossRef]
6. Lee, S.; Shah, Y.T. *Biofuels and Bioenergy: Processes and Technologies*; CRC Press: Boca Raton, FL, USA, 2012; ISBN 978-1-4200-8955-4.
7. Poletto, M. *Lignin: Trends and Applications*; BoD—Books on Demand: Norderstedt, Germany, 2018; ISBN 978-953-51-3901-0.
8. Pandey, M.P.; Kim, C.S. Lignin Depolymerization and Conversion: A Review of Thermochemical Methods. *Chem. Eng. Technol.* **2011**, *34*, 29–41. [CrossRef]
9. Holladay, J.E.; Bozell, J.J.; White, J.F.; Johnson, D. Results of Screening for Potential Candidates from Biorefinery Lignin. In *Top Value Added Candidates Biomass*; U.S. Department of Energy: Washington, DC, USA, 2007; pp. 53–55.
10. Sinha, S.; Jhalani, A.; Ravi, M.R.; Ray, A. Modelling of Pyrolysis in Wood: A Review. *SESI J.* **2000**, *10*, 41–62.
11. Guan, Q.; Mao, T.; Zhang, Q.; Miao, R.; Ning, P.; Gu, J.; Tian, S.; Chen, Q.; Chai, X.-S. Catalytic Gasification of Lignin with Ni/Al2O3–SiO2 in Sub/Supercritical Water. *J. Supercrit. Fluids* **2014**, *95*, 413–421. [CrossRef]
12. Barati, M.; Babatabar, M.; Tavasoli, A.; Dalai, A.K.; Das, U. Hydrogen Production via Supercritical Water Gasification of Bagasse Using Unpromoted and Zinc Promoted Ru/γ-Al2O3 Nanocatalysts. *Fuel Process. Technol.* **2014**, *123*, 140–148. [CrossRef]
13. Safari, F.; Tavasoli, A.; Ataei, A.; Choi, J.-K. Hydrogen and Syngas Production from Gasification of Lignocellulosic Biomass in Supercritical Water Media. *Int. J. Recycl. Org. Waste Agric.* **2015**, *4*, 121–125. [CrossRef]
14. Reddy, S.N.; Nanda, S.; Dalai, A.K.; Kozinski, J.A. Supercritical Water Gasification of Biomass for Hydrogen Production. *Int. J. Hydrog. Energy* **2014**, *39*, 6912–6926. [CrossRef]
15. Guo, L.J.; Lu, Y.J.; Zhang, X.M.; Ji, C.M.; Guan, Y.; Pei, A.X. Hydrogen Production by Biomass Gasification in Supercritical Water: A Systematic Experimental and Analytical Study. *Catal. Today* **2007**, *129*, 275–286. [CrossRef]
16. Saxena, R.C.; Seal, D.; Kumar, S.; Goyal, H.B. Thermo-Chemical Routes for Hydrogen Rich Gas from Biomass: A Review. *Renew. Sustain. Energy Rev.* **2008**, *12*, 1909–1927. [CrossRef]
17. Calzavara, Y.; Joussot-Dubien, C.; Boissonnet, G.; Sarrade, S. Evaluation of Biomass Gasification in Supercritical Water Process for Hydrogen Production. *Energy Convers. Manag.* **2005**, *46*, 615–631. [CrossRef]
18. Resende, F.L.P.; Savage, P.E. Kinetic Model for Noncatalytic Supercritical Water Gasification of Cellulose and Lignin. *AIChE J.* **2010**, *56*, 2412–2420. [CrossRef]
19. Pinkard, B.R.; Gorman, D.J.; Tiwari, K.; Rasmussen, E.G.; Kramlich, J.C.; Reinhall, P.G.; Novosselov, I.V. Supercritical Water Gasification: Practical Design Strategies and Operational Challenges for Lab-Scale, Continuous Flow Reactors. *Heliyon* **2019**, *5*, e01269. [CrossRef] [PubMed]
20. Yoshida, T.; Oshima, Y.; Matsumura, Y. Gasification of Biomass Model Compounds and Real Biomass in Supercritical Water. *Biomass Bioenergy* **2004**, *26*, 71–78. [CrossRef]
21. Yoshida, T.; Matsumura, Y. Gasification of Cellulose, Xylan, and Lignin Mixtures in Supercritical Water. *Ind. Eng. Chem. Res.* **2001**, *40*, 5469–5474. [CrossRef]
22. Van Duin, A.C.T.; Dasgupta, S.; Lorant, F.; Goddard, W.A. ReaxFF: A Reactive Force Field for Hydrocarbons. *J. Phys. Chem. A* **2001**, *105*, 9396–9409. [CrossRef]
23. Jin, H.; Wu, Y.; Guo, L.; Su, X. Molecular Dynamic Investigation on Hydrogen Production by Polycyclic Aromatic Hydrocarbon Gasification in Supercritical Water. *Int. J. Hydrog. Energy* **2016**, *41*, 3837–3843. [CrossRef]
24. Jin, H.; Wu, Y.; Zhu, C.; Guo, L.; Huang, J. Molecular Dynamic Investigation on Hydrogen Production by Furfural Gasification in Supercritical Water. *Int. J. Hydrog. Energy* **2016**, *41*, 16064–16069. [CrossRef]
25. Jin, H.; Chen, B.; Zhao, X.; Cao, C. Molecular Dynamic Simulation of Hydrogen Production by Catalytic Gasification of Key Intermediates of Biomass in Supercritical Water. *J. Energy Resour. Technol.* **2017**, 140. [CrossRef]
26. Rismiller, S.C.; Groves, M.M.; Meng, M.; Dong, Y.; Lin, J. Water Assisted Liquefaction of Lignocellulose Biomass by ReaxFF Based Molecular Dynamic Simulations. *Fuel* **2018**, *215*, 835–843. [CrossRef]
27. Zheng, M.; Wang, Z.; Li, X.; Qiao, X.; Song, W.; Guo, L. Initial Reaction Mechanisms of Cellulose Pyrolysis Revealed by ReaxFF Molecular Dynamics. *Fuel* **2016**, *177*, 130–141. [CrossRef]
28. Zhang, T.; Li, X.; Qiao, X.; Zheng, M.; Guo, L.; Song, W.; Lin, W. Initial Mechanisms for an Overall Behavior of Lignin Pyrolysis through Large-Scale ReaxFF Molecular Dynamics Simulations. *Energy Fuels* **2016**, *30*, 3140–3150. [CrossRef]
29. Zhang, T.; Li, X.; Guo, L.; Guo, X. Reaction Mechanisms in Pyrolysis of Hardwood, Softwood, and Kraft Lignin Revealed by ReaxFF MD Simulations. *Energy Fuels* **2019**, *33*, 11210–11225. [CrossRef]
30. Li, H.; Xu, B.; Jin, H.; Luo, K.; Fan, J. Molecular Dynamics Investigation on the Lignin Gasification in Supercritical Water. *Fuel Process. Technol.* **2019**, *192*, 203–209. [CrossRef]
31. Han, Y.; Chen, F.; Ma, T.; Gong, H.; Al-Shwafy, K.W.A.; Li, W.; Zhang, J.; Zhang, M. Size Effect of a Ni Nanocatalyst on Supercritical Water Gasification of Lignin by Reactive Molecular Dynamics Simulations. *Ind. Eng. Chem. Res.* **2019**, *58*, 23014–23024. [CrossRef]
32. Liu, X.; Wang, T.; Chu, J.; He, M.; Li, Q.; Zhang, Y. Understanding Lignin Gasification in Supercritical Water Using Reactive Molecular Dynamics Simulations. *Renew. Energy* **2020**, *161*, 858–866. [CrossRef]
33. Zakzeski, J.; Bruijnincx, P.C.A.; Jongerius, A.L.; Weckhuysen, B.M. The Catalytic Valorization of Lignin for the Production of Renewable Chemicals. *Chem. Rev.* **2010**, *110*, 3552–3599. [CrossRef]
34. Ponnuchamy, V.; Gordobil, O.; Diaz, R.H.; Sandak, A.; Sandak, J. Fractionation of Lignin Using Organic Solvents: A Combined Experimental and Theoretical Study. *Int. J. Biol. Macromol.* **2020**. [CrossRef]

35. Schmidt, M.W.; Baldridge, K.K.; Boatz, J.A.; Elbert, S.T.; Gordon, M.S.; Jensen, J.H.; Koseki, S.; Matsunaga, N.; Nguyen, K.A.; Su, S.; et al. General Atomic and Molecular Electronic Structure System. *J. Comput. Chem.* **1993**, *14*, 1347–1363. [CrossRef]
36. Zhang, Y.; He, H.; Dong, K.; Fan, M.; Zhang, S. A DFT Study on Lignin Dissolution in Imidazolium-Based Ionic Liquids. *RSC Adv.* **2017**, *7*, 12670–12681. [CrossRef]
37. Ju, Z.; Xiao, W.; Yao, X.; Tan, X.; Simmons, B.A.; Sale, K.L.; Sun, N. Theoretical Study on the Microscopic Mechanism of Lignin Solubilization in Keggin-Type Polyoxometalate Ionic Liquids. *Phys. Chem. Chem. Phys.* **2020**, *22*, 2878–2886. [CrossRef]
38. Melián-Rodríguez, M.; Saravanamurugan, S.; Meier, S.; Kegnæs, S.; Riisager, A. Ru-Catalyzed Oxidative Cleavage of Guaiacyl Glycerol-β-Guaiacyl Ether-a Representative β-O-4 Lignin Model Compound. *Catalysts* **2019**, *9*, 832. [CrossRef]
39. Zhu, Y.; Han, Z.; Fu, L.; Liu, C.; Zhang, D. Cleavage of the β–O–4 Bond in a Lignin Model Compound Using the Acidic Ionic Liquid 1-H-3-Methylimidazolium Chloride as Catalyst: A DFT Mechanistic Study. *J. Mol. Model.* **2018**, *24*, 322. [CrossRef] [PubMed]
40. Chen, M.; Zhong, W.; Wu, K.; Wei, G.; Hu, Z.; Zheng, W.; Ruan, H.; Zhang, H.; Xiao, R. Catalytic Pyrolysis Mechanism of β-O-4 Type of Lignin Dimer: The Role of H Proton. *Energy Fuels* **2021**, *35*, 575–582. [CrossRef]
41. Morales, G.; Iglesias, J.; Melero, J.A. Sustainable Catalytic Conversion of Biomass for the Production of Biofuels and Bioproducts. *Catalysts* **2020**, *10*, 581. [CrossRef]
42. Drage, T.C.; Vane, C.H.; Abbott, G.D. The Closed System Pyrolysis of β-O-4 Lignin Substructure Model Compounds. *Org. Geochem.* **2002**, *33*, 1523–1531. [CrossRef]
43. He, T.; Zhang, Y.; Zhu, Y.; Wen, W.; Pan, Y.; Wu, J.; Wu, J. Pyrolysis Mechanism Study of Lignin Model Compounds by Synchrotron Vacuum Ultraviolet Photoionization Mass Spectrometry. *Energy Fuels* **2016**, *30*, 2204–2208. [CrossRef]
44. Hu, B.; Zhang, B.; Xie, W.; Jiang, X.; Liu, J.; Lu, Q. Recent Progress in Quantum Chemistry Modeling on the Pyrolysis Mechanisms of Lignocellulosic Biomass. *Energy Fuels* **2020**, *34*, 10384–10440. [CrossRef]
45. Martínez, L.; Andrade, R.; Birgin, E.G.; Martínez, J.M. PACKMOL: A package for building initial configurations for molecular dynamics simulations. *J. Comput. Chem.* **2009**, *30*, 2157–2164. [CrossRef]
46. Chenoweth, K.; van Duin, A.C.T.; Goddard, W.A. ReaxFF Reactive Force Field for Molecular Dynamics Simulations of Hydrocarbon Oxidation. *J. Phys. Chem. A* **2008**, *112*, 1040–1053. [CrossRef] [PubMed]
47. Zeng, J.; Cao, L.; Chin, C.-H.; Ren, H.; Zhang, J.Z.H.; Zhu, T. ReacNetGenerator: An Automatic Reaction Network Generator for Reactive Molecular Dynamics Simulations. *Phys. Chem. Chem. Phys.* **2020**, *22*, 683–691. [CrossRef] [PubMed]
48. Kawamoto, H. Lignin Pyrolysis Reactions. *J. Wood Sci.* **2017**, *63*, 117–132. [CrossRef]
49. McGinty, D.; Letizia, C.S.; Api, A.M. Fragrance Material Review on 1,3-Benzodioxole-5-Propanol, α-Methyl-, 5-Acetate. *Food Chem. Toxicol.* **2012**, *50*, S330–S332. [CrossRef]
50. Pingali, S.R.K.; Jursic, B.S. Microwave-Assisted Synthesis of 1,3-Benzodioxole Derivatives from Catechol and Ketones or Aldehydes. *Tetrahedron Lett.* **2011**, *52*, 4371–4374. [CrossRef]
51. Zhu, C.; Guo, L.; Jin, H.; Ou, Z.; Wei, W.; Huang, J. Gasification of Guaiacol in Supercritical Water: Detailed Reaction Pathway and Mechanisms. *Int. J. Hydrog. Energy* **2018**, *43*, 14078–14086. [CrossRef]
52. Cao, C.; Xie, Y.; Li, L.; Wei, W.; Jin, H.; Wang, S.; Li, W. Supercritical Water Gasification of Lignin and Cellulose Catalyzed with Co-Precipitated CeO_2–ZrO_2. *Energy Fuels* **2021**. [CrossRef]
53. Miliotti, E.; Dell'Orco, S.; Lotti, G.; Rizzo, A.M.; Rosi, L.; Chiaramonti, D. Lignocellulosic Ethanol Biorefinery: Valorization of Lignin-Rich Stream through Hydrothermal Liquefaction. *Energies* **2019**, *12*, 723. [CrossRef]
54. Okuda, K.; Umetsu, M.; Takami, S.; Adschiri, T. Disassembly of Lignin and Chemical Recovery—Rapid Depolymerization of Lignin without Char Formation in Water–Phenol Mixtures. *Fuel Process. Technol.* **2004**, *85*, 803–813. [CrossRef]
55. Toledano, A.; Serrano, L.; Labidi, J. Improving Base Catalyzed Lignin Depolymerization by Avoiding Lignin Repolymerization. *Fuel* **2014**, *116*, 617–624. [CrossRef]
56. Chakar, F.S.; Ragauskas, A.J. Review of Current and Future Softwood Kraft Lignin Process Chemistry. *Ind. Crop. Prod.* **2004**, *20*, 131–141. [CrossRef]